# AM1 and PM3 Semiempirical Calculations on 1-Aryl-3,3-diethyltriazenes. Correlation of Bond Orders with Rotational Barriers and Quantum Yields of Photolysis

**J.-C. Panitz,[†] Th. Lippert,[†] J. Stebani,[‡] O. Nuyken,[‡,§] and A. Wokaun*,[†]**

*Physical Chemistry II and Macromolecular Chemistry I, University of Bayreuth, D-W-8580 Bayreuth, Germany*

*Received: January 6, 1993*

Molecular geometries, electronic transitions, bond orders, and dipole moments are calculated for 19 1-aryl-3,3-diethyltriazenes and two 3-alkyl-1,5-diarylpentazadienes, using standard AM1 and PM3 semiempirical methods. Calculated UV spectra compare well with the experimental results. A strong correlation is established between the barrier to internal rotation, $\Delta G^{\ddagger}$, and the $N^2$—$N^3$ bond order. The photochemical decomposition of substituted triazenes and pentazadienes is of interest in view of their application as promoters in laser-induced polymer ablation. Therefore, the photolysis quantum yields at 308 nm are investigated in various solvents. The influence of substituents on the aryl moiety on the quantum yield is analyzed in terms of a correlation with the calculated $N^1$=$N^2$ bond order. The effects of different nitrogen-bound alkyl substituents on the photochemical decomposition behavior can be represented by a similar correlation. Differences between the photolysis behavior of triazene and pentazadiene derivatives are discussed.

## Introduction

Recently, it has been found that 1,3-diphenyltriazene[1] and substituted 1-phenyl-3,3-dialkyltriazenes[2] can be effectively used as promoters in excimer laser-induced ablation of polymers. In order to obtain insight into the ablation mechanism, ground- and excited-state electronic properties of this class of compounds must be characterized.

The triazeno group, $-N^1{=}N^2{-}N^3-$, may be photolyzed according to either ionic or radical fragmentation pathways, depending on the substitution pattern, the resulting bond orders, and dipolar charge shifts within the N=N—N functionality. To obtain an experimental measure of bond orders, the restricted rotation around the $N^2$—$N^3$ bond of the triazene group has been studied by temperature-dependent NMR measurements.[3] In the present report, the activation energies derived from these measurements are correlated with bond orders obtained from semiempirical quantum chemical calculations.

The photochemical decomposition of the triazene compounds by 308-nm excimer laser irradiation is investigated in solution, and the corresponding quantum yields are determined for polar and nonpolar solvents. Electronic transition energies of 1-aryl-3,3-diethyltriazenes are calculated, and the results of the AM1 and PM3 parametrizations are compared with the experimental spectra. Ground- and excited-state electronic properties are correlated with the photolysis quantum yield.

Due to the fact that some triazenes exhibit pronounced antitumor activity, this class of compounds has received considerable attention.[4-6] In this context, Shusterman et al.[7] have studied the structure–activity relationship of substituted 1-phenyl-3,3-dimethyltriazenes. The authors found a correlation of mutagenicity in the Ames test with MNDO molecular orbital energies and the octanol–water partition coefficient.[7]

## Methods

**Investigated Compounds.** The synthesis of the investigated triazene compounds, as identified in Table I, has been described in ref 3. Pentazadienes were prepared according to the procedure described by Remes et al.;[8] details will be given at another place.

**TABLE I: Investigated Triazene and Pentazadiene Compounds**

| label | compound |
|---|---|
| 1 | 1-(3-carboxyphenyl)-3,3-diethyltriazene |
| 2 | 1-(3-carboxyphenyl)-3,3-di-*n*-propyltriazene |
| 3 | 1-(3-carboxyphenyl)-3,3-diisopropyltriazene |
| 4 | 1-(4-carboxyphenyl)-3,3-diethyltriazene |
| 5 | 1-(3,5-dicarboxyphenyl)-3,3-diethyltriazene |
| 6 | 1-(3,5-dicarboxyphenyl)-3,3-bis(2-hydroxyethyl)triazene |
| 7 | 1-(3,5-dicarboxyazidophenyl)-3,3-diethyltriazene |
| 8 | 1-(4-cyanophenyl)-3,3-diethyltriazene |
| 9 | 1-phenyl-3,3-diethyltriazene |
| 10 | 1-(4-methylphenyl)-3,3-diethyltriazene |
| 11 | 1-(2-methoxyphenyl)-3,3-diethyltriazene |
| 12 | 1-(3-methoxyphenyl)-3,3-diethyltriazene |
| 13 | 1-(4-methoxyphenyl)-3,3-diethyltriazene |
| 14 | 1-(2,4-dimethoxyphenyl)-3,3-diethyltriazene |
| 15 | 1-(2-nitrophenyl)-3,3-diethyltriazene |
| 16 | 1-(3-nitrophenyl)-3,3-diethyltriazene |
| 17 | 1-(4-nitrophenyl)-3,3-diethyltriazene |
| 18 | 1-(2,4-dinitrophenyl)-3,3-diethyltriazene |
| 19 | 1-(4-cyanophenyl)-3,3-dimethyltriazene |
| 20 | *syn*-1,5-bis(4-methoxyphenyl)-3-ethylpentazadiene |
| 21 | *anti*-1,5-bis(4-methoxyphenyl)-3-ethylpentazadiene |
| 22 | 1,5-bis(4-methylphenyl)-3-methylpentazadiene |

**UV–Visible Spectra.** UV spectra have been recorded on a conventional double-beam spectrophotometer (Perkin Elmer, Model Lambda 17). The triazene compounds were dissolved in various UV-grade solvents (cyclohexane, THF, methanol, or DMSO), with typical concentrations in the $1 \times 10^{-4}$ M range.

**Photolysis Experiments.** Solutions of the triazene compounds in the UV-grade solvents, at concentrations indicated above, were carefully degassed with Ar in standard 10-mm-thickness quartz cuvettes. For irradiation at 308 nm, the rectangular (10 mm × 20 mm) beam of a XeCl* excimer laser (Lambda Physik, Model LPX 100) was incident on a side face of the cuvette. Pulses of 120-mJ energy were delivered at a rate of 2 Hz. The extent of photolysis after a given number of pulses was followed off-line by recording the UV spectrum.

**Quantum Chemical Calculations.** Calculations have been carried out on DEC 5000/120 workstations (Digital Equipment Corp.). The semiempirical program package SCAMP 4.30,[9] which is based on the AMPAC 1.0[10] and MOPAC 4.0[11] programs,

* Author to whom correspondence should be addressed.
† Physical Chemistry II.
‡ Macromolecular Chemistry I.
§ Present address: Institute of Technical Chemistry, Technical University of Munich, D-W-8046 Garching.

0022-3654/93/2097-5246$04.00/0 © 1993 American Chemical Society

was used in all calculations. For each compound, computations were carried out with both the AM1[12] and the PM3[13] parametrizations. Input files were conveniently generated with SHOWMOLE;[14] the latter program is also used to process the output files.

Molecular geometries were fully optimized without imposing any idealizations or symmetry relations. To check whether the geometries obtained did indeed represent true stationary points, force constant calculations have been performed which yield the vibrational frequencies, as well as the eigenvalues corresponding to translation. In each case, it was verified[15] that all eigenvalues were positive for the final structure.

The molecular structures obtained in this way were used in a configurational interaction calculation to compute dipole moments, bond orders, and electronic transition energies. Oscillator strengths were computed using the SCAMP keyword INTENS.

## Results

**Molecular Geometry.** Semiempirical calculations have been performed for the compounds given in Table I. Geometry optimization was checked for two compounds by comparison of calculated parameters with known crystallographic data, i.e., for 1-(4-cyanophenyl)-3,3-dimethyltriazene (**19**) and for 1,5-bis(4-methylphenyl)-3-methylpentazadiene (**22**).

Fronczek et al.[16] reported that **19** crystallizes in the monoclinic space group $P2_1/c$, with four formula units per unit cell. The triazene functional group is twisted out of the plane of the phenyl moiety; a significant "quinoidal" shortening of C–C bonds in the aromatic ring is observed.[16] Both AM1 and PM3 calculations are well capable of reproducing these experimental results. The geometry of **19**, as calculated with the AM1 parametrization, is shown in Figure 1a. Calculated and experimental bond lengths are compared in Table II. Only distances between the heavy atoms have been included, taking into account the well-known fact that hydrogen positions determined by X-ray methods are subject to considerable uncertainties.

The quality of geometry optimization has been judged from the sum of squared deviations between measured and calculated bond lengths. It was found that

$$\sum(r_{\mathrm{AM1}} - r_{\mathrm{exp}})^2 = 34\ \mathrm{pm}^2 \quad \text{and} \quad \sum(r_{\mathrm{PM3}} - r_{\mathrm{exp}})^2 = 113\ \mathrm{pm}^2$$

The corresponding standard deviations are 1.7 and 3.1 pm, respectively. Bond lengths in the aromatic ring calculated by the PM3 method agree almost perfectly with the experimental values. However, on the overall average the AM1 model appears to better reproduce the X-ray geometry. With respect to bond angles, the standard deviation between calculation and experiment amounts to 3.1° and 3.2° for AM1 and PM3 parametrizations, respectively. For the dihedral angles, the standard deviations are 9.2° and 9.3°, respectively.

These accuracies may be compared with the average errors reported by Stewart,[15] who has tested the MOPAC parametrizations with a large number of compounds. The author indicates the following average errors: bond lengths, 5.0 pm with AM1 and 3.6 pm with PM3; bond angles, 3.3° with AM1 and 3.9° with PM3; dihedral angles, 12.5° with AM1 and 14.9° with PM3, where the data set used for the comparison of dihedral angles was considered too small for statistical significance.[15] Thus, the agreement between experimental and calculated geometries obtained for compound **19** compares favorably with the accuracy that may be expected for the semiempirical technique employed.

The same comparison was carried out for selected bond lengths in the reference compound 1,5-bis(4-methylphenyl)-3-methylpentazadiene (**22**, cf. Figure 1a). This compound crystallizes in the orthorhombic space group *Pccn*, with four formula units per unit cell.[17] For the 11 different skeleton bonds, the sum of squared deviation of bond lengths amounts to 34 pm$^2$ when using the AM1 model. The PM3 method leads to a value of 55 pm$^2$. Thus, with respect to geometric parameters, AM1 appears to be the method of choice for both types of compounds.

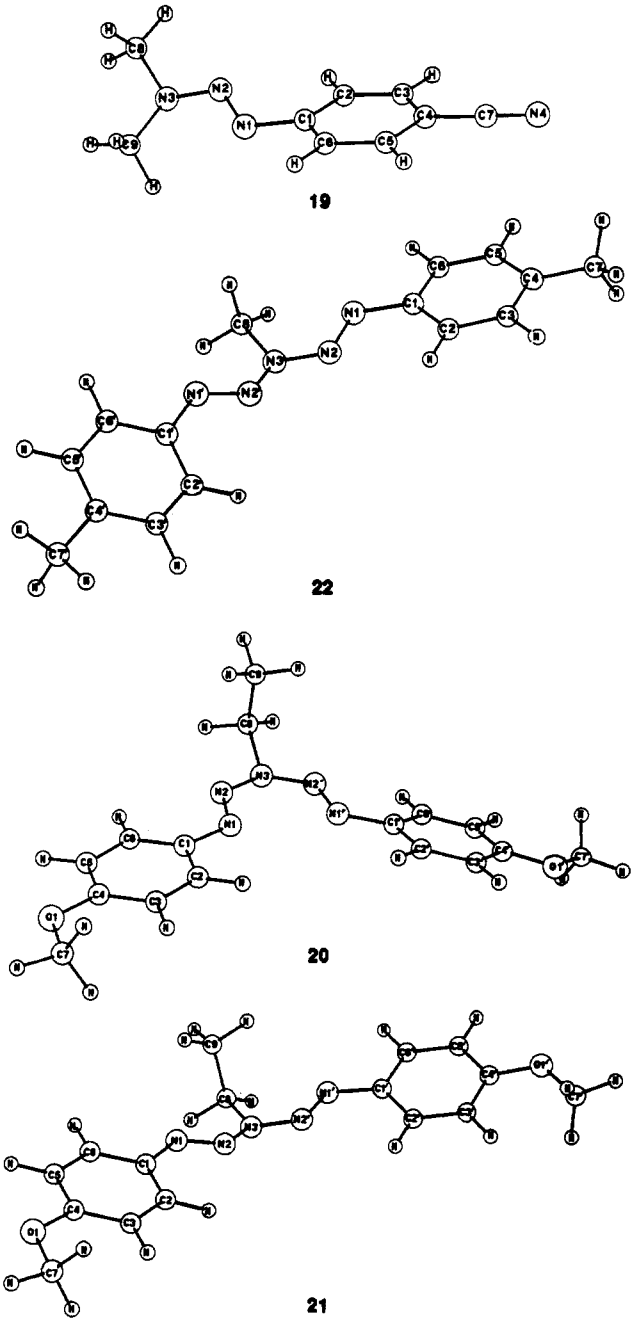


**Figure 1.** (a, top) Structural formulas of the reference compounds 1-(4-cyanophenyl)-3,3-dimethyltriazene (**19**) and 1,5-bis(4-methylphenyl)-3-methylpentazadiene (**22**). The labels of the atoms are the same as in Table II, where experimental and calculated bond lengths are given. (b, bottom) Structural formulas of *syn*-1,5-bis(4-methoxyphenyl)-3-ethylpentazadiene (**20**) and *anti*-1,5-bis(4-methoxyphenyl)-3-ethylpentazadiene (**21**). The geometries shown represent the equilibrium structures obtained from the AM1 calculations described in the text.

**Pentazadienes: Stereoisomers.** The ground state of the compound 1,5-bis(4-methoxyphenyl)-3-ethylpentazadiene has been studied using the geometry parameters obtained with compound **13** as an input. This approach leads to a final geometry (compound **20**) shown in Figure 1b, which may be designated as a syn rotamer with respect to the $N^3$–$N^2$ bond. Noting that our reference compound, **22**, is known to crystallize in the anti conformation with respect to the equivalent bond (cf. Figure 1a), a calculation has also been performed for the energy minimum

**TABLE II: Comparison of Bond Lengths[a] from the Present Calculation and from X-ray Diffraction**

| | AM1 | PM3 | exp |
|---|---|---|---|
| 1-(4-Cyanophenyl)-3,3-dimethyltriazene (**19**) | | | |
| C6–C1 | 141.3 | 140.1 | 139.3[b] |
| C1–C2 | 141.0 | 139.9 | 140.1 |
| C2–C3 | 139.1 | 139.0 | 137.8 |
| C3–C4 | 140.1 | 139.7 | 139.6 |
| C4–C5 | 140.2 | 139.8 | 139.2 |
| C5–C6 | 138.9 | 138.8 | 138.0 |
| C4–C7 | 142.1 | 142.5 | 143.9 |
| C7–N4 | 116.4 | 116.0 | 113.9 |
| C1–N1 | 142.8 | 144.5 | 141.8 |
| N1–N2 | 124.6 | 123.7 | 127.0 |
| N2–N3 | 133.6 | 138.3 | 131.6 |
| N3–C8 | 146.0 | 148.9 | 144.5 |
| N3–C9 | 145.8 | 148.8 | 144.2 |
| 1,5-Bis(4-methylphenyl)-3-methylpentazadiene (**22**) | | | |
| C1–C6 | 138.7 | 140.9 | 139.9[c] |
| C1–C2 | 138.6 | 141.3 | 140.1 |
| C2–C3 | 138.3 | 138.9 | 138.8 |
| C3–C4 | 138.7 | 140.0 | 139.7 |
| C4–C5 | 138.9 | 139.8 | 139.6 |
| C5–C6 | 138.7 | 139.2 | 138.9 |
| C1–N1 | 142.9 | 143.0 | 144.4 |
| N1–N2 | 126.4 | 123.9 | 123.3 |
| N2–N3 | 136.1 | 137.0 | 139.8 |
| N3–C8 | 145.2 | 147.7 | 149.6 |
| C4–C7 | 150.5 | 148.0 | 148.5 |

[a] In pm. [b] Reference 14. [c] Reference 15.

**TABLE III: Calculated and Experimental Dipole Moments[a]**

| compd | AM1 | PM3 | exp[b] |
|---|---|---|---|
| **10** | 1.496 | 1.429 | 1.95 |
| **9** | 1.754 | 1.732 | |
| **13** | 1.829 | 1.461 | |
| **15** | 4.543 | 4.561 | 4.31 |
| **4** | 4.696 | 4.487 | |
| **8** | 5.172 | 4.689 | |
| **19** | 5.347 | 4.794 | |
| **17** | 8.074 | 8.017 | 7.04 |
| **22** | 0.655 | 0.858 | |

[a] In D (debye). [b] For the corresponding 1-aryl-3,3-dimethyltriazenes, from ref 18.

that corresponds to the anti rotamer of **20**. The resulting structure (**21**) is included in Figure 1b.

Concerning the total energy differences, the AM1 and PM3 calculations lead to completely different results. With the AM1 Hamiltonian, the syn conformer is *significantly* more stable than the anti conformer, with the total energy difference amounting to 24.7 kJ/mol. In contrast, the PM3 parametrization renders the anti rotamer more stable, with a smaller total energy difference of 6.4 kJ/mol.

In agreement with chemical intuition, X-ray diffraction[17] shows that the reference compound **22** is present in the anti conformation in the crystal, which would support the result obtained using the PM3 parametrization. We recall that the influence of the surrounding medium is not taken into account on the level of the SCAMP program package. It is therefore of interest to acquire spectroscopic information on the conformational equilibrium between syn and anti forms in solution. According to AM1, only the syn conformer should be present at room temperature, whereas from the PM3 result, the syn:anti ratio would amount to 7:93.

**Dipole Moments.** Dipole moments have been calculated for all investigated compounds; some results are shown in Table III. Data on the physical properties of triazenes are relatively scarce in the literature; to our knowledge, only three values of experimental dipole moments have been reported that could be compared with our calculated results. These values were determined with *N,N-dimethyl*-substituted triazenes.[18] For a valid comparison, we have to assume that a change of the alkyl substituents does not result in strong alteration of the charge distribution. This assumption is justified by inspection of the calculated dipole moments (Table III) of compounds **8** and **19**, which differ only in the alkyl substitution. The reported values differ only by a few percent.

With this in mind, the calculated dipole moments for triazene compounds **10**, **15**, and **17** may be compared with the experimental values in Table III. We conclude that both the AM1 and PM3 models provide good estimates of the actual values, within 0.5 D or within 10% for the most polar compound.

**Electronic Excitation Energies.** Wavelengths and oscillator strengths of electronic transitions have been calculated for the investigated triazene and pentazadiene compounds; the AM1 results are compiled in Table IV. Representative results for 1-(4-nitrophenyl)- and 1-(3-carboxyphenyl)-3,3-diethyltriazene are compared with the experimental spectra recorded in cyclohexane solution. Inspection of Figures 2 and 3 shows that transition energies are reproduced more accurately by the AM1 model. On the other hand, the PM3 calculations give a better account of the oscillator strength, i.e., the intensity pattern. These trends are confirmed for the entire series of compounds. For both methods, the agreement between calculated and experimental spectra is quite satisfactory. This is demonstrated in Figure 4, where the calculated stick spectrum obtained with the AM1 parametrization has been convoluted by Lorentzian line profiles, of 1500-$cm^{-1}$ fwhm.

**N=N Bond Orders.** As a characteristic feature, the electronic charge distribution of 1-phenyl-3,3-dialkyltriazene compounds contains a 1,3 dipolar component, in which charge is shifted from the lone pair of the alkyl nitrogen ($N^3$) onto the nitrogen atom $N^1$. As a consequence, the $N^3$—$N^2$ bond acquires partial double bond character, and the $N^2$=$N^1$ bond order is <2. Results for the calculated $N^3$—$N^2$ and $N^2$—$N^1$ bond orders are summarized in Table V.

**Photolysis Quantum Yields.** Quantum yields for 308-nm irradiation in cyclohexane, tetrahydrofuran (THF), methanol, and dimethyl sulfoxide have been determined for five para-substituted and four meta-substituted 1-phenyl-3,3-diethyltriazene compounds, as well as for the pentazadiene compounds. Results are compiled in Table VI and will be discussed below.

For a few of the solutions, it was found that the photolysis quantum yield was not constant during an experimental run on a given sample but decreased with the number of pulses delivered to the sample. This indicates that photolysis products are interfering either by absorbing the incident laser photons or by acting as quenchers. In these exceptional cases, average quantum yields over the course of photolysis are indicated.

For most of the compounds, the dependence of the long wavelength absorption maximum around 300 nm on the solvent is weak, i.e., shifts are of the order of 5 nm. The *p*-cyano- and *p*-nitro derivatives (**8** and **17**, respectively) represent a remarkable exception. Here, a change of the solvent from cyclohexane to dimethyl sulfoxide results in a blue shift by ≈20 nm.

The 308-nm photolysis of the pentazadiene compound **21** appears to proceed in a one-step reaction on the time scale of our experimental setup. In this respect, the photochemical behavior is similar to that of the triazene compounds. However, the quantum yield of decomposition of **21** upon 308-nm irradiation in THF amounts to ≈20%; i.e., 1 order of magnitude higher than observed with the triazene derivatives.

As expected, a significant dependence of the photolysis quantum yield on the irradiation wavelength is observed. Furthermore, for some of the compounds an influence of temperature on the quantum yield was noticed. Quantification of these effects is in progress in our laboratory.

## Discussion

**Correlation between $N^2$–$N^3$ Bond Order and Internal Rotation Barrier.** In an NMR study[3] of hindered internal rotation around

**TABLE IV: Calculated Wavelengths λ[a] and Oscillator Strengths *f* of Electronic Transitions**

| compd | λ | *f* | λ | *f* | λ | *f* | λ | *f* | λ | *f* | λ | *f* | λ | *f* |
|---|---|---|---|---|---|---|---|---|---|---|---|---|---|---|
| **1** | 330 | 0.061 | 315 | 0.020 | 300 | 0.278 | 270 | 0.096 | 238 | 0.419 | 218 | 0.167 | 216 | 0.443 |
| **2** | 333 | 0.054 | 315 | 0.022 | 300 | 0.280 | 269 | 0.106 | 237 | 0.441 | 218 | 0.146 | 216 | 0.441 |
| **3** | 321 | 0.129 | 315 | 0.011 | 295 | 0.195 | 283 | 0.008 | 248 | 0.464 | 225 | 0.276 | 216 | 0.443 |
| **4** | 346 | 0.093 | 304 | 0.011 | 303 | 0.359 | 272 | 0.027 | 239 | 0.236 | 224 | 0.279 | 209 | 0.655 |
| **5** | 326 | 0.072 | 310 | 0.024 | 300 | 0.278 | 265 | 0.282 | 231 | 0.236 | 218 | 0.255 | 216 | 0.499 |
| **6** | 326 | 0.032 | 307 | 0.024 | 300 | 0.294 | 263 | 0.249 | 231 | 0.349 | 216 | 0.482 | 216 | 0.316 |
| **8** | 347 | 0.079 | 304 | 0.037 | 303 | 0.340 | 265 | 0.011 | 245 | 0.376 | 218 | 0.006 | 207 | 0.702 |
| **9** | 359 | 0.018 | 304 | 0.001 | 296 | 0.297 | 276 | 0.011 | 248 | 0.209 | 223 | 0.507 | 220 | 0.043 |
| **10** | 359 | 0.025 | 308 | 0.002 | 302 | 0.338 | 277 | 0.012 | 249 | 0.193 | 222 | 0.493 | 226 | 0.074 |
| **11** | 362 | 0.017 | 313 | 0.002 | 295 | 0.164 | 278 | 0.031 | 252 | 0.339 | 227 | 0.419 | 215 | 0.150 |
| **12** | 362 | 0.019 | 321 | 0.011 | 298 | 0.206 | 276 | 0.035 | 256 | 0.375 | 226 | 0.516 | 221 | 0.199 |
| **13** | 354 | 0.033 | 311 | 0.011 | 307 | 0.371 | 275 | 0.013 | 249 | 0.163 | 221 | 0.571 | 205 | 0.725 |
| **14** | 372 | 0.038 | 325 | 0.026 | 306 | 0.202 | 278 | 0.037 | 253 | 0.308 | 231 | 0.218 | 225 | 0.466 |
| **15** | 327 | 0.115 | 313 | 0.010 | 289 | 0.130 | | | 249 | 0.530 | 225 | 0.383 | 211 | 0.145 |
| **16** | | | 318 | 0.044 | 306 | 0.186 | 277 | 0.045 | 248 | 0.644 | 219 | 0.389 | 217 | 0.016 |
| **17** | 324 | 0.285 | 300 | 0.001 | 291 | 0.189 | | | 236 | 0.367 | 209 | 0.468 | 212 | 0.175 |
| **18** | 328 | 0.309 | 307 | 0.006 | 294 | 0.146 | | | 242 | 0.348 | 226 | 0.400 | 213 | 0.194 |
| **21** | 324 | 0.947 | 291 | 0.061 | 289 | 0.069 | 283 | 0.069 | 221 | 0.246 | 212 | 0.288 | | |
| **7** | 264 | 0.003 | 258 | 0.029 | 239 | 0.004 | 228 | 0.878 | 224 | 0.868 | 210 | 0.003 | | |

[a] Calculated using the AM1 parametrization; wavelengths in nm. Only transitions with λ > 200 nm are included in the table.

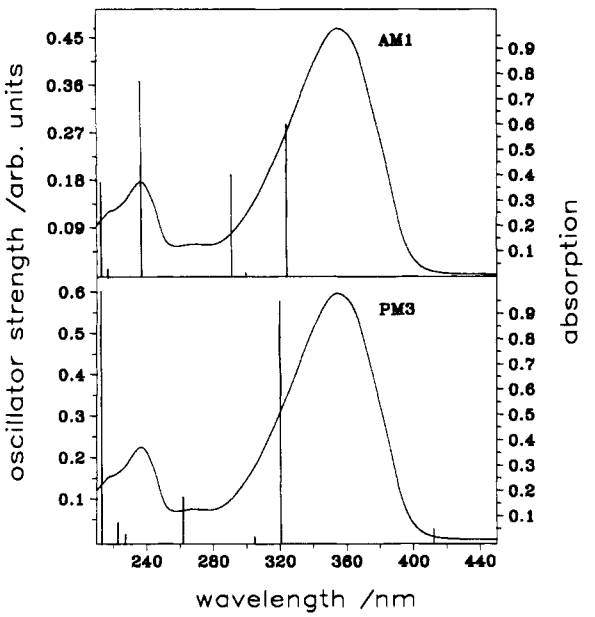


**Figure 2.** Absorption spectrum of 1-(4-nitrophenyl)-3,3-diethyltriazene (**19**). The experimental spectrum (solid line) is compared with the transition energies and oscillator strengths calculated using the AM1 parametrization (stick spectrum, upper diagram) and using the PM3 parametrization (stick spectrum, lower diagram).

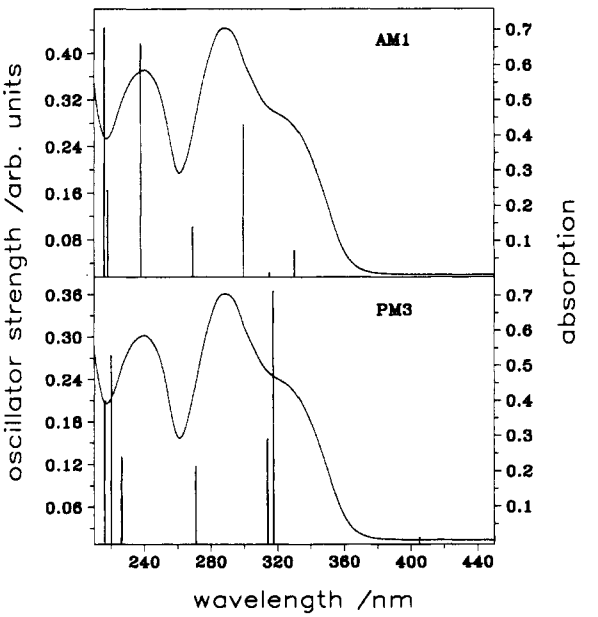


**Figure 3.** Absorption spectrum of 1-(3-carboxyphenyl)-3,3-diethyltriazene (**1**). The experimental spectrum (solid line) is compared with the transition energies and oscillator strengths calculated using the AM1 parametrization (stick spectrum, upper diagram) and using the PM3 parametrization (stick spectrum, lower diagram).

the $N^3$–$N^2$ bond, we have argued that the height of the barrier to internal rotation, and hence the activation energy, is correlated with the electronic charge distribution and the bond orders in the triazeno group. The free energy of rotation $\Delta G^{\ddagger}$, as determined from NMR,[3] is plotted against the calculated $N^2$–$N^3$ bond order in Figure 5. A significant correlation is indeed obtained if the two groups of para- and meta-substituted triazene derivatives are considered separately. The corresponding linear regressions, as shown in Figure 5, are characterized by correlation coefficients, *r*, of 0.925.

Bond-order changes have been interpreted in terms of a 1,3 shift of electronic charge, i.e., the involvement of a 1,3 dipolar resonance structure. In classical chemical notation, this could be represented as $N^1{=}N^2{-}N^3 \leftrightarrow {}^-N^1{-}N^2{=}N^{3+}$. The importance of such a structure might be judged from atomic charges obtained in the molecular orbital (MO) calculation. The AM1 parametrization fails to reproduce the 1,3 dipolar shift. In contrast, with PM3 the charge redistribution is clearly seen, and its magnitude is readily extracted from the atomic charges. In agreement with expectations from Figure 5, the charge separation in the triazeno group is larger with **17** (4-nitrophenyl substituent) than with **13** (4-methoxyphenyl substituent).

As a consequence of charge transfer from the alkyl substituents onto $N^3$, additional negative charge ($\approx -0.08e_0$) is accumulated at this nitrogen atom. This partial charge is determined by the alkyl substituents and may be considered separately from the charge shift induced by the phenyl substituent at $N^1$. The latter turns out to correspond to a symmetric dipole, with a negative partial charge at $N^1$ and an opposite charge of similar magnitude at $N^3$. From the partial charges, the contribution of the 1,3 dipolar mesomeric resonance structure is estimated to correspond to about 10%.

**Quantum Yields of Photolysis.** To interpret the differences in quantum yields reported in Table VI, the correlation of this quantity with the $N^1{=}N^2$ bond order is tested. A survey plot for the four different solvents used is presented in Figure 6. Meaningful correlations are only obtained if the investigated compounds are classified according to their substitution pattern. For the para compounds, the correlation of quantum yield with bond order is due to the different electronic effects of the varied

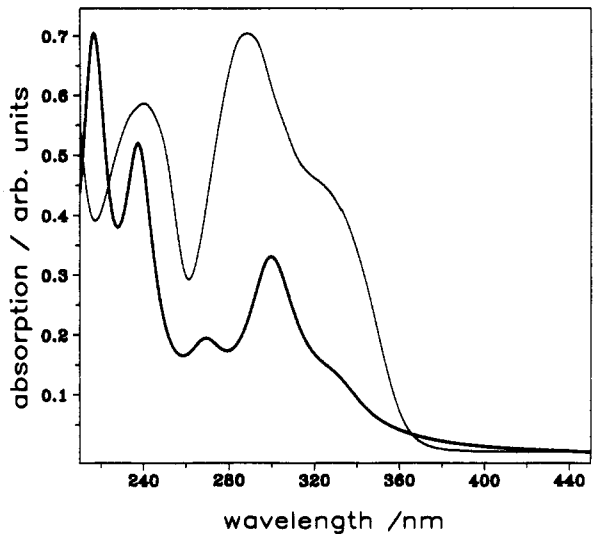


**Figure 4.** Absorption spectrum of 1-(3-carboxyphenyl)-3,3-diethyltriazene (**1**). The experimental spectrum is represented by the thin solid line. For the calculated spectrum (bold solid line), Lorentzian profiles of 1500-$cm^{-1}$ fwhm have been centered at the wavelengths of the relevant electronic transitions, with the relative intensities determined by the corresponding oscillator strengths. The AM1 parametrization has been used in the calculation of the electronic transitions.

**TABLE V: Calculated[a] Bond Orders in the Triazene Group[b]**

| compd | C1–N1 | N1–N2 | N2–N3 |
|---|---|---|---|
| **1** | 1.021 | 1.744 | 1.122 |
| **2** | 1.022 | 1.743 | 1.123 |
| **3** | 1.022 | 1.725 | 1.140 |
| **4** | 1.023 | 1.742 | 1.127 |
| **5** | 1.023 | 1.736 | 1.134 |
| **6** | 1.021 | 1.752 | 1.116 |
| **7** | 1.020 | 1.745 | 1.127 |
| **8** | 1.024 | 1.739 | 1.128 |
| **9** | 1.017 | 1.760 | 1.105 |
| **10** | 1.018 | 1.761 | 1.103 |
| **11** | 1.012 | 1.769 | 1.104 |
| **12** | 1.017 | 1.756 | 1.111 |
| **13** | 1.021 | 1.762 | 1.098 |
| **14** | 1.014 | 1.782 | 1.091 |
| **15** | 1.028 | 1.734 | 1.142 |
| **16** | 1.025 | 1.730 | 1.139 |
| **17** | 1.030 | 1.723 | 1.146 |
| **18** | 1.052 | 1.683 | 1.187 |
| **19** | 1.022 | 1.748 | 1.122 |
| **20** | 1.015 | 1.829 | 1.009 |
| **21** | 1.016 | 1.816 | 1.027 |
| **22** | 1.01 | 1.817 | 1.027 |

[a] Using the AM1 parametrization. [b] Numbering of atoms is the same as in Figure 1.

substituents. In contrast, the investigated meta-substituted triazene derivatives all contain one (two) COOH substituents in the 3 (3,5) position on the aromatic ring, while the alkyl substituents at nitrogen atom $N^3$ are varied.

Inspection of Figure 6 and Table VI reveals that, once the grouping into para- and meta-substituted derivatives has been taken into account, the correlation between photolysis quantum yield and $N^1{=}N^2$ bond order is fair for the two polar solvents methanol and dimethyl sulfoxide. An increase in $N^1{=}N^2$ bond strength, which is accompanied by a decrease in $N^2{-}N^3$ bond order, appears to favor the photolytic cleavage of the comparatively weaker $N^2{-}N^3$ bond. In contrast, correlations are much poorer for the less polar solvents cyclohexane and THF, where the quantum yield might well be termed independent of $N^1{=}N^2$ bond order. We note that, in general, the quantum yields are higher in the nonpolar solvents. Acid-substituted triazene derivatives, for which the quantum yields are highest in methanol, represent an exception.

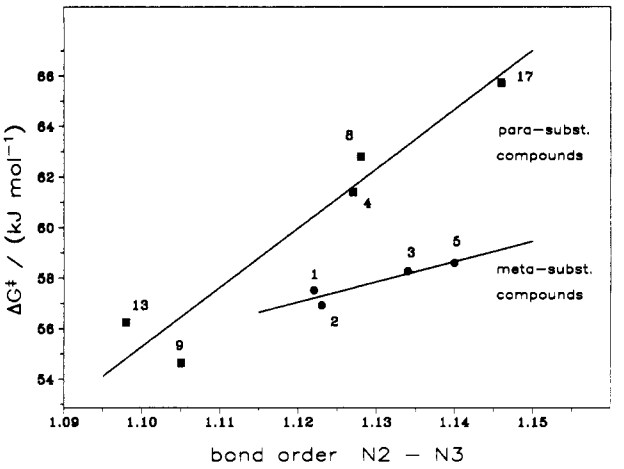


**Figure 5.** Correlation of free energy of internal rotation, $\Delta G^{\ddagger}$, with the $N^2$–$N^3$ bond order computed in the AM1 parametrization. Linear correlations (solid lines) have been computed for a set of five para-substituted triazenes (squares) and for four meta-substituted compounds (circles).

As the NMR data have also been recorded in methanol, we shall concentrate on this solvent. The quantum yields of 308-nm photolysis in methanol are analyzed in more detail in Figure 7. For the five para-substituted compounds in which the phenyl substituent is varied, a correlation coefficient, $r$, of 0.92 is obtained. For the series of four meta-substituted compounds with variation of the alkyl substituent, $r = 0.87$. Baro et al.[19] have stated that methanol is thought to provide comparably stable solvent cages for the cis–trans isomerization of dissolved diphenyltriazene molecules, as a consequence of the network of hydrogen bonds that exists in liquid methanol. If the radicals produced upon photolysis cannot escape the solvent cage, the influence of intramolecular effects on the decomposition behavior is expected to be more pronounced than in a solvent environment of labile structure.

In this and the preceding section, it has been stated that $\Delta G^{\ddagger}$ and photolysis quantum yield are related to $N^2{-}N^3$ and $N^1{=}N^2$ bond orders, respectively. (We note from Table V that a decrease in $N^1{=}N^2$ bond order is always accompanied by an approximately equal and opposite increase in $N^2{-}N^3$ bond order.) An obvious further test for the validity of these correlations can be performed by plotting quantum yield and $\Delta G^{\ddagger}$ against each other, as shown in Figure 8 for the subset of the para-substituted triazenes. Again, a clear linear correlation with $r = 0.9$ is obtained.

For the pentazadiene **21**, the $N^1{=}N^2$ bond order is significantly increased as compared to the similarly substituted triazene compound **13**, whereas the $N^2{-}N^3$ bond order is reduced. If we assume that photochemical decomposition of the pentazadienes proceeds by a similar mechanism as found with the triazenes, the quantum yield of pentazadiene photolysis should be larger. Experimentally, this is indeed observed (Table VI). From the linear correlation between quantum yield and $N^1{=}N^2$ bond order mentioned above, a quantum yield of 1.9% is estimated, which is larger than observed with the triazenes but smaller than the experimental value by more than 1 order of magnitude. This comparison indicates that, for the highly reactive pentazadienes, other factors are important in addition, which will be the subject of further studies.

Bugaeva and Kondratenko[20] have also determined photolysis quantum yields between 20% and 30% of pentazadiene compounds; from their calculations, the authors conclude that photochemical dissociation is faster by 1 order of magnitude than relaxation by trans–cis isomerization. This behavior constitutes a pronounced difference from the behavior of triazene compounds, where the energy barrier to internal rotation around the $N^2{-}N^3$ bond is significantly smaller.

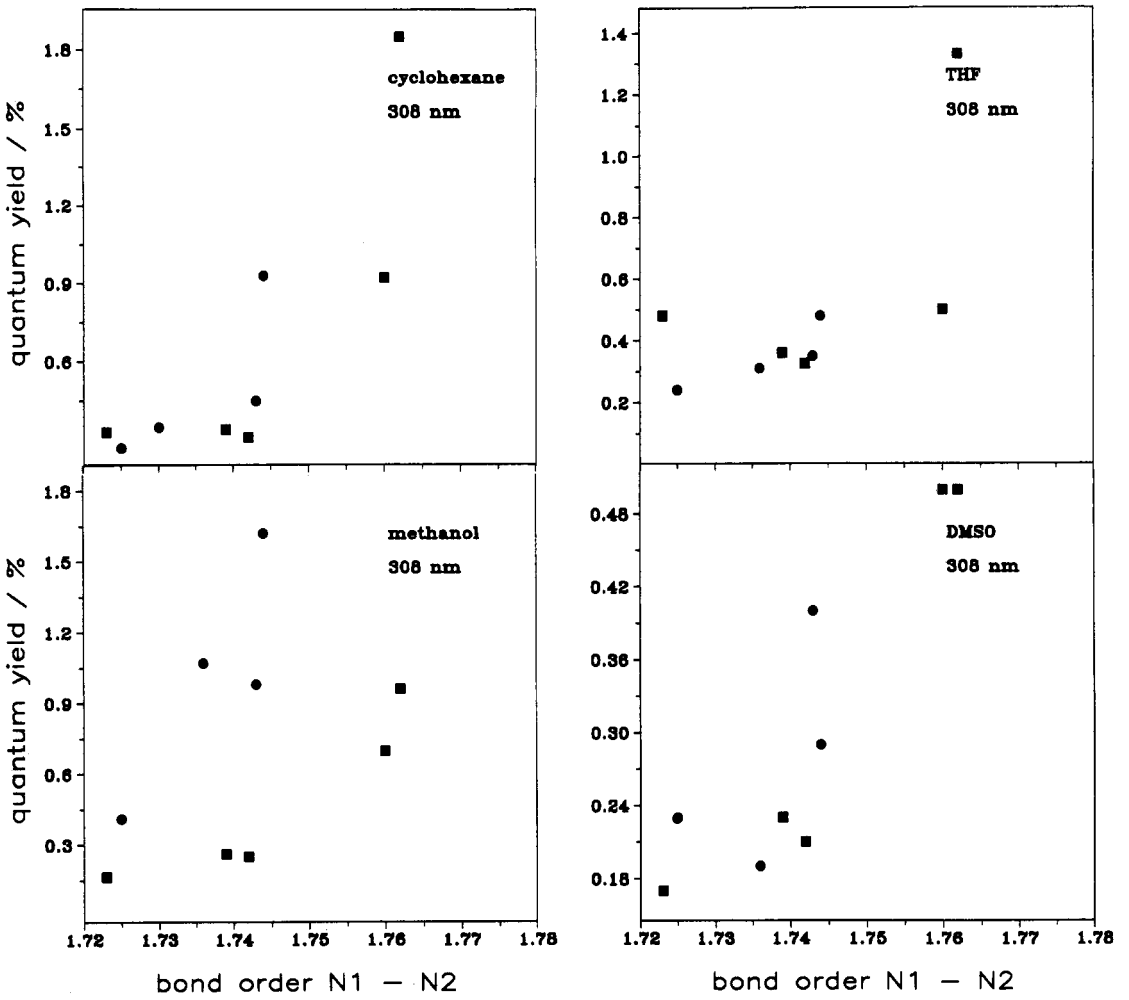


**Figure 6.** Correlation of the photolysis quantum yield with the $N^1{=}N^2$ bond order computed in the AM1 parametrization. Scatter plots are shown for the four solvents cyclohexane, tetrahydrofuran (THF), methanol, and dimethyl sulfoxide (DMSO). Meta- and parasubstituted triazene derivatives are designated by circles and squares, respectively. The detailed assignment to the individual compounds is given in Table VI and in Figure 7.

**TABLE VI: Quantum Yields for 308-nm Photolysis of Triazene Compounds**

| compound | phenyl substituent | alkyl substituent | quantum yield in solvent (%) $C_6H_{12}$[a] | $C_4H_8O$[b] | $CH_3OH$ | $(CH_3)_2SO$ | bond order[c] |
|---|---|---|---|---|---|---|---|
| **1** | 3-COOH | $C_2H_5$ | 0.92 | 0.48 | 1.62 | 0.29 | 1.744 |
| **2** | 3-COOH | $n$-$C_3H_7$ | 0.44 | 0.35 | 0.98 | 0.40 | 1.743 |
| **3** | 3-COOH | $i$-$C_3H_7$ | 0.26 | 0.24 | 0.41 | 0.23 | 1.725 |
| **5** | 3,5-COOH | $C_2H_5$ | – | 0.31 | 1.07 | 0.19 | 1.736 |
| **4** | 4-COOH | $C_2H_5$ | 0.31 | 0.33 | 0.25 | 0.21 | 1.742 |
| **8** | 4-CN | $C_2H_5$ | 0.34 | 0.36 | 0.26 | 0.23 | 1.739 |
| **9** | 4-H | $C_2H_5$ | 0.92 | 0.50 | 0.70 | 0.50 | 1.760 |
| **13** | 4-$OCH_3$ | $C_2H_5$ | 1.85 | 1.33 | 0.96 | 0.50 | 1.762 |
| **17** | 4-$NO_2$ | $C_2H_5$ | 0.33 | 0.48 | 0.16 | 0.17 | 1.723 |
| **21** | 4-$OCH_3$ (pentazadiene) | $C_2H_5$ | 15.1 | 21.0 | 31.2 | | |

Coefficients of Linear Regression Analysis[d]

| position of phenyl substituent | solvent $C_6H_{12}$[a] | $C_4H_8O$[b] | $CH_3OH$ | $(CH_3)_2SO$ | position of phenyl substituent | solvent $C_6H_{12}$[a] | $C_4H_8O$[b] | $CH_3OH$ | $(CH_3)_2SO$ |
|---|---|---|---|---|---|---|---|---|---|
| *para* | | | | | *meta* | | | | |
| intercept $a$ | −56.6 | – | −33.9 | −16.3 | intercept $a$ | – | −16.8 | −83.8 | – |
| slope $b$ | 32.9 | – | 19.7 | 9.5 | slope $b$ | – | 9.9 | 48.8 | – |
| correl coeff $r$ | 0.80 | 0.59 | 0.92 | 0.94 | correl coeff $r$ | 0.74 | 0.86 | 0.87 | 0.62 |

[a] Cyclohexane. [b] Tetrahydrofuran. [c] $N^1{=}N^2$. [d] Quantum yield = $a + b$(bond order $N^1{=}N^2$).

**Analysis of the Lowest Electronic Transitions.** The highest occupied MO of the electronic ground state, as well as the two lowest unoccupied molecular orbitals, are experiencing the most important changes in orbital occupation number during the strong UV transition around 300 nm. As these orbitals have always a dominant $p_z$ character, the latter excitation can be assigned to a $\pi \rightarrow \pi^*$ transition.

Due to the configurational interaction approach taken to compute the UV transition energies, an interpretation regarding the characters of the respective transitions is by no means simple. The UV transitions contain at least three, and up to seven, significant contributions from different transitions between molecular orbitals located below or above the HOMO (disregarding the different spin states).

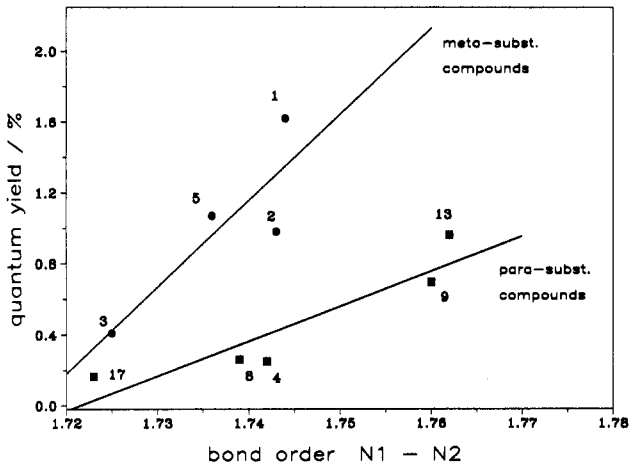


**Figure 7.** Correlation of the photolysis quantum yield in methanol with the $N^1{=}N^2$ bond order obtained with the AM1 model. Linear correlations (solid lines) have been computed for a set of five para-substituted triazenes (squares) and for four meta-substituted compounds (circles). The triazene derivatives are identified by their labels; cf. Table I.

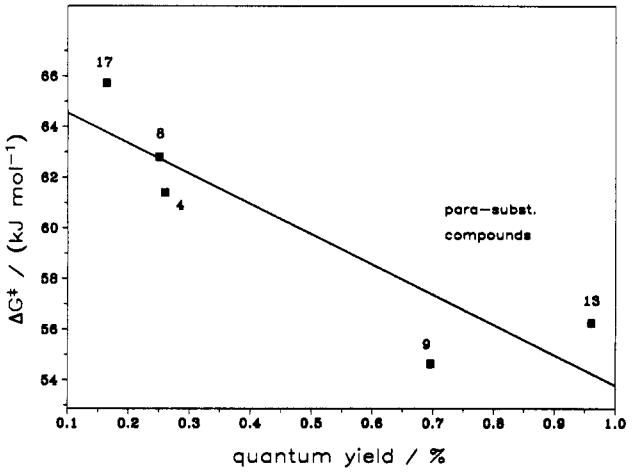


**Figure 8.** Correlation of the free energy of internal rotation around the $N^2$–$N^3$ bond, $\Delta G^{\ddagger}$, with the quantum yield of photolysis in methanol. Data are shown for the five para-substituted triazene derivatives in Table VI.

Nevertheless, valuable information can be extracted from a close inspection of the eigenvectors that constitute the excited-state wave functions. This is exemplified for the case of the three principal UV transitions of compound **17**, 1-(4-nitrophenyl)-3,3-diethyltriazene, with calculated wavelengths of 324, 291, and 236 nm, respectively. Referring to Table VII, we see that for the transition at 324 nm, the two most dominant contributions are the HOMO → LUMO and the (HOMO – 1) → LUMO excitations. Inspection of the eigenvectors reveals that this absorption can be interpreted as a $\pi \rightarrow \pi^*$ transition. The orbital pictures generated with the program SHOWMOLE (Figure 9) demonstate that this electronic excitation involves a charge transfer from the triazeno group to the phenyl ring and to the *p*-nitro substituent.

A large contribution to the absorption at 236 nm consists of a (HOMO – 2) → (LUMO + 1) transition. These orbitals are almost exclusively localized on the phenyl ring; they represent $\pi$-bonding and $\pi$-antibonding orbitals with respect to the two bonds for which a quinoidal shortening has been observed both in the X-ray structure and in the calculations, as mentioned above. The orbitals also correspond to the HOMO and LUMO of benzene and have been designated as $\Phi$ and $\Phi^*$, respectively, by Helfferich et al.[21] Therefore, the (HOMO – 2) → (LUMO + 1) transition can be assigned to the $\Phi \rightarrow \Phi^*$ excitation in the nomenclature of ref 21. In addition, the above-mentioned charge transfer from the triazeno group to the nitro substituent contributes significantly to the 236-nm transition.

**TABLE VII: Analysis of the Principal UV Transitions of 1-(4-Nitrophenyl)-3,3-diethyltriazene (17)**

| λ/nm | orbital excitation | contribution/% |
|---|---|---|
| 324 | HOMO → LUMO | 50.0 |
| | HOMO – 1 → LUMO | 27.0 |
| | HOMO – 1 → LUMO + 2 | 6.8 |
| | HOMO – 2 → LUMO + 1 | 6.5 |
| | HOMO – 3 → LUMO + 2 | 4.4 |
| | HOMO → LUMO + 2 | 3.7 |
| | sum | 98.4 |
| 291 | HOMO → LUMO | 29.7 |
| | HOMO – 1 → LUMO | 28.4 |
| | HOMO – 1 → LUMO + 2 | 20.0 |
| | HOMO – 3 → LUMO | 15.2 |
| | HOMO – 2 → LUMO + 1 | 4.0 |
| | sum | 96.8 |
| 236 | HOMO – 2 → LUMO + 1 | 42.8 |
| | HOMO – 3 → LUMO | 23.6 |
| | HOMO → LUMO + 2 | 12.0 |
| | HOMO → LUMO | 8.4 |
| | HOMO – 1 → LUMO | 7.8 |
| | HOMO → LUMO[a] | 1.1 |
| | sum | 95.7 |

[a] Both electrons are excited.

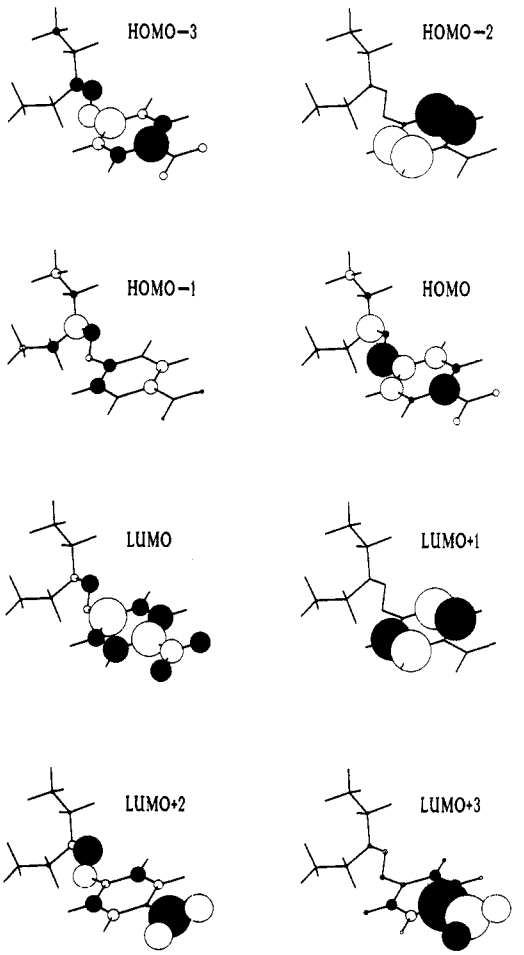


**Figure 9.** Orbital coefficients at atomic centers for the molecular orbitals involved in the electronic transitions of compound **1**. The four occupied orbitals which are highest in energy, (HOMO – 3) ... HOMO, and the four unoccupied orbitals with the lowest energy, LUMO ... (LUMO + 3), are displayed. Orbital coefficients of opposite sign are displayed by open and filled circles. The radius of each circle is proportional to the coefficient of the corresponding $p_z$ orbital; the area of the circle is thus proportional to the $p_z$ orbital population. For the (LUMO + 3) orbital, the sum of all valence orbital coefficients is displayed.

## Conclusions

The present study shows that electronic transitions of substituted 1-phenyl-3,3-dialkyltriazene compounds, which contain ≈15 heavy atoms on average, can be calculated with good accuracy using the semiempirical AM1 method. The UV spectra in the 200–400-nm region are well reproduced by the calculations. As a consequence of extensive state mixing in the configurational interaction, several one-electron excitations are contributing significantly to the lowest energy absorptions. Among these, a $\pi \rightarrow \pi^*$ excitation resulting in a charge transfer from the triazeno group onto the aromatic ring and a $\Phi \rightarrow \Phi^*$ excitation within the aromatic ring system can be clearly identified.

The bond order of the formal single bond $N^2$–$N^3$ is increased as a consequence of a 1,3 dipolar electronic charge distribution. The calculated bond order is significantly correlated with the energy barrier to internal rotation as derived from NMR, i.e., the free energy $\Delta G^*$. On the other hand, the quantum yield of photolysis at 308 nm is strongly correlated with the $N^1{=}N^2$ bond order. This correlation was established for para-substituted triazenes in which the substituent at the phenyl moiety was varied and for a series of meta-substituted derivatives in which the influence of alkyl substituents at $N^3$ was tested.

The quantum yield of photolysis is found to be a sensitive function of both substituent type and substitution pattern. The correlations obtained could therefore be used to predict photolysis quantum yields for further triazene compounds. Furthermore, they might be helpful in understanding the mechanism of photolysis. To this aim, the changes in the electronic structure involved in the photolytical bond cleavage and ejection of nitrogen will be analyzed by further calculations, which are currently in progress.

**Acknowledgment.** The authors express their sincere gratitude to T. Clark (University of Erlangen) for stimulating discussions and for making the SCAMP program package available. Financial support of this work by the Deutsche Forschungsgemeinschaft (SFB 213) and by the Verband der Chemischen Industrie is gratefully acknowledged.

## References and Notes

(1) Bolle, M.; Luther, K.; Troe, J.; Ihlemann, J.; Gerhardt, H. *Appl. Surf. Sci.* **1990**, *46*, 279.
(2) Lippert, Th.; Stebani, J.; Nuyken, O.; Wokaun, A.; Ihlemann, J., unpublished manuscript.
(3) Lippert, Th.; Dauth, J.; Nuyken, O.; Wokaun, A. *Magn. Res. Chem.* **1992**, *30*, 1178.
(4) Wilman, D. E. V. *Magn. Reson. Chem.* **1990**, *28*, 729.
(5) Foster, B. J.; Newell, D. R.; Carmichael, J.; Harris, A. L.; Grumbrell, L. A.; Wilman, D. E. V.; Calvert, A. H. *Brit. J. Cancer* **1988**, *58*, 276.
(6) Giraldi, T.; Connors, T. A.; Carter, G., Eds. *Triazenes, Chemical, Biological, and Clinical Aspects*; Plenum: New York, 1990.
(7) Shusterman, A. J.; Johnson, A. S.; Hansch, C. *Int. J. Quantum. Chem.* **1989**, *36*, 19.
(8) Remes, M.; Divis, J.; Zverina, V.; Matrka, M. *Chem. Prum.* **1973**, *23*, 133.
(9) Clark, T. University of Erlangen, 1990.
(10) Liotard, D. A.; Healy, E. F.; Ruiz, J. M.; Dewar, M. J. S. AMPAC, Program 506, Quantum Chemistry Program Exchange, University of Indiana, Bloomington, IN.
(11) Stewart, J. J. P. MOPAC, Program 455, Quantum Chemistry Program Exchange, University of Indiana, Bloomington, IN.
(12) Dewar, M. J. S.; Zoebisch, E. G.; Healy, E. F.; Stewart, J. J. P. *J. Am. Chem. Soc.* **1985**, *107*, 3902.
(13) Stewart, J. J. P. *J. Comput. Chem.* **1989**, *10*, 209, 221. Stewart, J. J. P. *J. Comput. Aided Mol. Design* **1990**, *4*, 1.
(14) Herrmann, F.; Kerber, A.; Wokaun, A. SHOWMOLE, University of Bayreuth, 1991.
(15) Stewart, J. J. P. In *Reviews in Computational Chemistry*; Lipkowitz, K. B., Boyd, D. B., Eds.; VCH: Weinheim, 1990; p 45.
(16) Fronczek, F. R.; Hansch, C.; Watkins, S. F. *Acta Crystallogr.* **1988**, *C44*, 1651.
(17) Beck, J. *Z. Naturforsch.* **1988**, *43B*, 1219.
(18) LeFevre, R. J. W.; Liddicoet, T. H. *J. Chem. Soc.* **1951**, 2743.
(19) Baro, J.; Dudek, D.; Luther, K.; Troe, J. *Ber. Bunsenges. Phys. Chem.* **1983**, *87*, 1155.
(20) Bugaeva, L. N.; Kondratenko, P. A. *Fundam. Osnovy. Optich. Pamyati i Sredy, Kiev* **1989**, *20*, 86; *Chem. Abstr. 112*(14), 128933e. Bugaeva, L. N.; Kondratenko, P. A. *Zh. Prikl. Spektrosk.* **1990**, *53*, 286; *Chem. Abstr.* **1990**, *113*(20), 181200k.
(21) van Beek, L. K. H.; Helfferich, J.; Houtman, H. J.; Jonker, H. *Recueil* **1967**, *86*, 977.